12-1-2015

Bisphosphonate Induces Osteonecrosis of the Jaw in Diabetic Mice via NLRP3/Caspase-1-Dependent IL-1β Mechanism

Qunzhou Zhang
University of Pennsylvania

Weihua Yu
University of Pennsylvania

Sumin Lee
University of Pennsylvania

Qilin Xu
University of Pennsylvania

Ali Naji
University of Pennsylvania

See next page for additional authors

Recommended Citation

Bisphosphonate Induces Osteonecrosis of the Jaw in Diabetic Mice via NLRP3/Caspase-1-Dependent IL-1**β** Mechanism

Abstract

Diabetes mellitus is an established risk factor associated with bisphosphonate-related osteonecrosis of the jaw (BRONJ). Sustained activation of Nod-like receptor (NLR) family, pyrin domain-containing protein 3 (NLRP3) inflammasome contributes to the persistent inflammation and impaired cutaneous wound healing in diabetic mice and human. We have recently demonstrated a compelling linkage between M1 macrophages and BRONJ conditions in both murine and human diseases. The aim of this study was to determine whether NLRP3 inflammasome activation is involved in BRONJ development in diabetic mice. We showed an increased incidence of delayed oral wound healing and bone necrosis of extraction sockets in db/db mice compared with those in nondiabetic db/+ controls, which correlated with an elevated expression of NLRP3, caspase-1, and IL-1β in macrophages residing at local wounds. Constitutively, bone marrow-derived macrophages from db/db mice (db/db BMDMs) secrete a relatively higher level of IL-1β than those from db/+ mice (db/+ BMDMs). Upon stimulation by NLRP3 activators, the secretion of IL-1β by db/db BMDMs was 1.77-fold higher than that by db/+ BMDMs (p < 0.001). Systemic treatment of mice with zoledronate (Zol), a nitrogen-containing bisphosphonate, resulted in a 1.86- and 1.63-fold increase in NLRP3/caspase-1-dependent IL-1β secretion by db/+ and db/db BMDMs, respectively, compared with BMDMs derived from nontreated mice (p < 0.001). Importantly, systemic administration of pharmacological inhibitors of NLRP3 activation improved oral wound healing and suppressed BRONJ formation in db/db mice. Mechanistically, we showed that supplementation with intermediate metabolites of the mevalonate pathway, inhibitors of caspase-1 and NLRP3 activation, an antagonist for P2X7R, or a scavenger of reactive oxygen species (ROS), robustly abolished Zol-enhanced IL-1β release from macrophages in response to NLRP3 activation (p < 0.001). Our findings suggest that diabetes-associated chronic inflammatory response may have contributed to impaired socket wound healing and rendered oral wound susceptible to the development of BRONJ via NLRP3 activation in macrophages. © 2015 American Society for Bone and Mineral Research.

Keywords

Disciplines

Dentistry | Oral and Maxillofacial Surgery | Oral Biology and Oral Pathology

Author(s)

Qunzhou Zhang, Weihua Yu, Sumin Lee, Qilin Xu, Ali Naji, and Anh D. Le

Bisphosphonate Induces Osteonecrosis of the Jaw in Diabetic Mice via NLRP3/Caspase-1-Dependent IL-1β Mechanism

Qunzhou Zhang,[1] Weihua Yu,[1] Sumin Lee,[1] Qilin Xu,[1] Ali Naji,[2] and Anh D Le[1,3]

[1]Department of Oral and Maxillofacial Surgery and Pharmacology, University of Pennsylvania School of Dental Medicine, Philadelphia, PA, USA
[2]Division of Transplantation, Department of Surgery, Perelman School of Medicine at the University of Pennsylvania, Philadelphia, PA, USA
[3]Department of Oral and Maxillofacial Surgery, Penn Medicine Hospital of the University of Pennsylvania, Philadelphia, PA, USA

ABSTRACT

Diabetes mellitus is an established risk factor associated with bisphosphonate-related osteonecrosis of the jaw (BRONJ). Sustained activation of Nod-like receptor (NLR) family, pyrin domain-containing protein 3 (NLRP3) inflammasome contributes to the persistent inflammation and impaired cutaneous wound healing in diabetic mice and human. We have recently demonstrated a compelling linkage between M1 macrophages and BRONJ conditions in both murine and human diseases. The aim of this study was to determine whether NLRP3 inflammasome activation is involved in BRONJ development in diabetic mice. We showed an increased incidence of delayed oral wound healing and bone necrosis of extraction sockets in db/db mice compared with those in nondiabetic $db/+$ controls, which correlated with an elevated expression of NLRP3, caspase-1, and IL-1β in macrophages residing at local wounds. Constitutively, bone marrow-derived macrophages from db/db mice (db/db BMDMs) secrete a relatively higher level of IL-1β than those from $db/+$ mice ($db/+$ BMDMs). Upon stimulation by NLRP3 activators, the secretion of IL-1β by db/db BMDMs was 1.77-fold higher than that by $db/+$ BMDMs ($p < 0.001$). Systemic treatment of mice with zoledronate (Zol), a nitrogen-containing bisphosphonate, resulted in a 1.86- and 1.63-fold increase in NLRP3/caspase-1-dependent IL-1β secretion by $db/+$ and db/db BMDMs, respectively, compared with BMDMs derived from nontreated mice ($p < 0.001$). Importantly, systemic administration of pharmacological inhibitors of NLRP3 activation improved oral wound healing and suppressed BRONJ formation in db/db mice. Mechanistically, we showed that supplementation with intermediate metabolites of the mevalonate pathway, inhibitors of caspase-1 and NLRP3 activation, an antagonist for P2X$_7$R, or a scavenger of reactive oxygen species (ROS), robustly abolished Zol-enhanced IL-1β release from macrophages in response to NLRP3 activation ($p < 0.001$). Our findings suggest that diabetes-associated chronic inflammatory response may have contributed to impaired socket wound healing and rendered oral wound susceptible to the development of BRONJ via NLRP3 activation in macrophages. © 2015 American Society for Bone and Mineral Research.

KEY WORDS: DIABETES; BISPHOSPHONATE; OSTEONECROSIS OF THE JAW; BRONJ; NLRP3

Introduction

Osteonecrosis of the jaw (ONJ), a condition of exposed/necrotic bone in the maxillofacial bone, is associated with antiresorptive therapies such as bisphosphonates and denosumab, a monoclonal antibody against human receptor activator of NF-κB ligand (RANKL).[1,2] Clinically, a majority of the cases of bisphosphonate-related osteonecrosis of the jaw (BRONJ) have been reported in cancer patients receiving high doses of intravenous (iv) nitrogen-containing bisphosphonates.[1,3] Even though several risk factors such as surgical or traumatic insults, oral infection, chemotherapeutic, anti-angiogenic agents, and steroids have been implicated in the pathogenesis of BRONJ, the etiology of this complication is still largely unknown.[1,4]

Diabetes-associated impaired wound healing represents a significant health problem and economic burden with millions of patients afflicted worldwide.[5] Numerous oral complications such as delayed wound healing after tooth extraction, alveolar bone resorption, and impaired bone formation around dental implants have been associated with diabetes mellitus.[6–9] Epidemiological evidence has implied that diabetes, especially type 2 diabetes, is also an important risk factor in the pathogenesis of ONJ.[10–13] The presence of diabetes or impaired fasting glucose apparently correlates with a higher prevalence of microvascular disease in diabetic BRONJ patients compared with diabetic controls.[11] BRONJ patients with diabetes experienced an impaired healing and a longer median time to heal compared with patients without this comorbidity.[14] However,

there is a lack of direct evidence demonstrating how this metabolic disease contributes to the underlying pathophysiology of BRONJ.

Nod-like receptor (NLR) family, pyrin domain-containing protein 3 (NLRP3) inflammasome plays a key role in innate immunity by activating caspase-1 and processing the pro-interleukin-1β (IL-1β) into the active cytokines.[15–17] Usually, the full activation of NLRP3 inflammasome requires two distinct signals. The first or "priming" signals are most commonly provided by pattern recognition receptors, eg, Toll-like receptors (TLRs), which activate the transcription of pro-IL-1β and NLRP3 through NF-κB pathway. The second signal is likely mediated by danger-associated molecular pattern molecules (DAMPs) such as ATP, uric acid, and reactive oxygen species (ROS), which lead to the assembly of NLRP3 inflammasome complex and the subsequent caspase-1 activation and IL-1β secretion.[15–17] Macrophages play an important role in innate immune responses, which can be polarized into two distinct phenotypes, the classically activated (M1) and the alternatively activated (M2) macrophages. Generally, M1 macrophages are characterized by the production of inflammatory mediators such as nitric oxide (NO), reactive oxygen species (ROS), interleukin (IL)-12, and tumor necrosis factor (TNF)-α, whereas M2 macrophages are characterized by the production of anti-inflammatory cytokines, such as IL-10 and transforming growth factor (TGF)-β, thus contributing to inflammation resolution and tissue modeling.[18,19] NLRP3 activation is usually present in M1 macrophages, not in M2 macrophages. In diabetic chronic wounds, an elevated IL-1β production in pro-inflammatory monocytes/macrophages dominates the local wound site,[20,21] and the sustained inflammasome activity in wound macrophages contributes to diabetes-associated impaired wound healing.[22–24] These findings suggest that activation of the NLRP3 cascade plays a critical role in aberrant wound healing and fibrosis in diabetes.[16] However, whether NLRP3 inflammasome activity contributes to abnormal oral wound healing, particularly the development of BRONJ, remains elusive.

Bisphosphonates, currently the most important class of antiresorptive agents, exert their potent inhibitory effects on osteoclast activity by blocking the mevalonate metabolic pathway.[25] In addition, monocytes and macrophages have also been shown to be the target cells of bisphosphonates.[26,27] Nitrogen-containing bisphosphonates, particularly zoledronate (Zol), could polarize M2-like tumor-associated macrophages toward an M1 phenotype and enhance proinflammatory cytokine production.[28,29] Importantly, mevalonate kinase deficiency has been linked to metabolic autoinflammatory disease,[30] and inhibition of mevalonate pathway by statins or nitrogen-containing bisphosphonates leads to NLRP3 activation in monocytes/macrophages.[31–35] Most recently, we have reported a compelling linkage between IL-17-mediated polarization of M1 macrophages and the development of BRONJ in both human disease and murine models.[36] In the present study, we utilized db/db mice, an established type 2 diabetic mouse model, to test our hypothesis that a persistent inflammation mediated by constitutive NLRP3 activation in macrophages contributes to diabetes-associated delayed oral socket healing and promotes BRONJ development in diabetic patients. Our findings indicate that diabetes-associated chronic inflammatory response may have contributed to impaired socket wound healing and rendered oral wound susceptible to the development of BRONJ via NLRP3 activation in macrophages.

Materials and Methods

Animal care

Mice and all animal procedures were handled according to the guidelines of the Institutional Animal Care and Use Committee (IACUC) of University of Pennsylvania. We followed a randomized, prospective, and controlled animal model design according to all the recommendations of the ARRIVE (Animal Research: Reporting In Vivo Experiments) guidelines (Kilkenny and colleagues). BKS.Cg-Dock7^m+/+Lepr^{db}/J mouse (db/db) is a well-established diabetic model caused by a single autosomal recessive mutation of the leptin receptor gene (Lepr^{db}) on chromosome 4 and displays phenotypes such as obesity, hyperglycemia, and impaired skin wound healing similar to those of patients with type 2 diabetes (http://jaxmice.jax.org/strain/000642.html). Diabetic db/db mice, nondiabetic db/+ control (male, 6 to 8 weeks old), and B6.129S6-Nlrp3^{tm1Bhk}/J (Nlrp3$^{-/-}$) mice were obtained from the Jackson Laboratory (Bar Harbor, ME, USA). Mice were group-housed in polycarbonate cages (three to five per cage) in the animal facilities with controlled temperature (23°C ± 2°C), 40% to 65% of humidity, and a 12-hour light/dark cycle. Mice were acclimatized for at least 1 week before the study, fed with a standard laboratory diet, and allowed ad libitum access to drinking water throughout the study.

Reagents and antibodies

Zoledronate (Zol) was generously provided by Novartis Pharma AG (CH-4002 Basel, Switzerland). Murine macrophage colony-stimulating factor (M-CSF) was purchased from PeproTech (Rocky Hill, NJ, USA). Lipopolysaccharide (LPS) from Escherichia coli 055:B5, nigericin, adenosine triphosphate (ATP), phorbol 12-myristate 13-acetate (PMA), farnesyl pyrophosphate (FPP) and geranylgeranyl pyrophosphate (GGPP), Ac-YVAD-CMK, glyburide, A438079, CA-074-Me, and N-acetyl-cysteine (NAC) were from Sigma (St. Louis, MO, USA). Antibodies for human and mice NLRP3 were from Sigma and Novus Biologicals (Littleton, CO, USA), respectively. Antibodies for human and mouse caspase-1 p10 (M-20) were from Santa Cruz (Dallas, TX, USA).

Cell culture

Human THP-1 monocyte and murine macrophage J774.A1 cell lines were obtained from ATCC (Manassas, VA, USA). THP-1 cells were cultured in RPMI-1640 medium supplemented with 10% fetal bovine serum (FBS) (Clontech, Mountain View, CA, USA), 10 mM glutamine, 100 U/mL penicillin, and 100 μg/mL streptomycin (Life Technologies, Carlsbad, CA, USA). J774.A1 cells were cultured in complete DMEM supplemented with 10% FBS, 100 U/mL penicillin, and 100 μg/mL streptomycin. Murine bone marrow-derived macrophages (BMDMs) were isolated and cultured as described previously.[36] Briefly, nucleated bone marrow cells were seeded at 2×10^6/well onto 6-well tissue culture plates and incubated at 37°C for 3 hours, and then nonadherent cells were removed by washing with PBS. The adherent cells were continuously cultured in complete DMEM containing 10 ng/mL murine M-CSF (PeproTech) for 6 days. Cell cultures were maintained in a humidified incubator with 5% CO_2 at 37°C.

Induction of BRONJ-like lesion in db/db diabetic mice

The BRONJ-like lesions in mice were induced according to the protocol we reported recently.[36,37] Briefly, db/db or db/+ mice

were randomly divided into zoledronate (Zol)-treated and nontreated control groups ($n = 8$). Mice from the treatment group were intravenously injected with Zol via the tail vein at a dose of 125 μg/kg twice a week, whereas animals from the nontreatment group were intravenously injected with 200 μL PBS. One week after Zol injection, the first maxillary molar teeth were extracted under deep anesthesia by intraperitoneal injection of ketamine (100 mg/kg) and xylazine (10 mg/kg). A total of 6 and 10 doses of zoledronate were administered for the 2- and 4-week follow-up groups, respectively. Sixteen of *db/+* and 32 of *db/db* mice were used for this experiment. To observe the therapeutic effect of blocking NLRP3 inflammasome activity on oral socket wound healing and BRONJ development in *db/db* mice, Zol-treated and nontreated animals were randomly grouped and treated with either glyburide or Ac-YVAD-cmk, a specific caspapse-1 inhibitor, whereas mice treated with vehicle were used as control ($n = 10$, 60 in total). Both drugs were prepared in 20% dimethyl sulfoxide (DMSO) and intraperitoneally (ip) administered at a dose of 50 mg/kg for glyburide (Sigma) once daily[38] and 5 mg/kg for Ac-YVAD-cmk (Sigma) twice a week, respectively. The body weight of animals was monitored twice a week, and the plasma glucose levels were recorded weekly from the tail vein blood using the Accu-Chek Aviva glucometer (Roche Diagnostics, Mannheim, Germany). Clinical evaluation of extracted tooth socket and determination of the incidence of BRONJ-like lesions were performed according to previous publications.[36,37]

Microcomputed tomography (μCT)

Intact and unprocessed maxilla specimens were scanned using a μCT machine at the Small Animal Imaging Facility (SAIF) of the Perelman School of Medicine at the University of Pennsylvania. Multisliced CT sections (5 to 10 microns thick), specifically at the tooth extraction regions corresponding to the first molars, were collected and analyzed as reported.[37]

Histological and immunohistochemical studies

Tissues were fixed with 4% PFA in PBS (pH 7.4) and decalcified with 5% EDTA in PBS (pH 7.4). Eight-μm-thick paraffin-embedded sections of bone samples were cut for H&E staining and immunohistochemical (IHC) studies using specific primary antibodies for NLRP3 (Novus Biologicals), cleaved casapse-1 (Santa Cruz), and IL-1β (Cell Signaling, Danvers, MA, USA) (1:200). For dual-color immunofluorescence studies, sections were immunostained with specific antibodies for a murine macrophage marker F4/80, NLRP3, caspase-1, and IL-1β (1:200), followed by staining with FITC- and rhodamine-conjugated secondary antibodies (1:400). Nuclei were stained with DAPI. Isotype-matched control antibodies (BioLegend, San Diego, CA, USA) were used as negative controls. Semiquantitative analysis of at least 5 sections per sample was performed in a blinded fashion. Positive signals in at least six random high-power fields (HPF) per section were visualized, counted, and expressed as the percentage of total nuclei cells.[36]

NLRP3 inflammasome activation

To determine the effect of Zol on NLRP3 activation, J774.A1 cells, murine BMDMs, or THP-1 monocytes were seeded in 12-well culture plates (5×10^5/well) and pretreated with different concentrations of Zol for 24 hours. Then NLRP3 activation was induced using the canonical two-signal model system. Briefly,

cells pretreated with Zol were primed with 200 ng/mL of purified lipopolysaccharide (LPS) for 4 hours as the first signal to induce the production of pro-IL-1β. Subsequently, the primed cells were stimulated with a second signal, either by 5 mM ATP for 4 hours or by 20 μM nigericin (a microbial toxin derived from *Streptomyces hygroscopicus* acting as a potassium ionophore) for 30 minutes.[39] Under certain conditions, THP-1 monocytes seeded in 12-well culture plates (5×10^5/well) were differentiated with phorbol 12-myristate acetate (PMA) (100 ng/mL) for 3 hours, which serves as the first signal, followed by treatment with different concentrations of Zol for 24 hours and stimulation with 5 mM ATP for another 4 hours. Both cells and culture supernatants were collected for immunoblots and ELISA, respectively.

Western blot analysis

Cell lysates were separated on polyacrylamide-SDS gel and electroblotted onto nitrocellulose membrane (Bio-Rad, Hercules, CA, USA). After blocking with 5% nonfat dry milk, the membrane was incubated with antibodies against NLRP3 or cleaved caspase-1, followed by incubation with a horseradish peroxidase (HRP)-conjugated secondary antibody. The signals were visualized by enhanced chemiluminescence (ECL) detection (Thermo Scientific, Waltham, MA, USA). The blots were reprobed with a specific antibody against β-actin as internal controls (GeneTex, Irvine, CA, USA).

ELISA

The concentration of IL-1β and IL-17 in mice serum or supernatants of cultured cells was detected using ELISA kits (BioLegend) according to the manufacturer's protocol.

Statistical analysis

All data are presented as mean ± standard deviation and tests of statistical hypotheses were performed by multifactorial analysis of variance, followed by Tukey's adjusted multiple pairwise comparisons (post hoc) tests using the ANOVA command of Stata statistical software program (StataCorp, 2013, Stata Statistical Software: Release 13, College Station, TX, USA). Values of $p < 0.05$ were considered statistically significant.

Results

Incidence of BRONJ was markedly increased in *db/db* mice

Initially, we explored the potential role of NLRP3 activation in BRONJ development in type 2 diabetic *db/db* mice induced by intravenous treatment with Zol (Fig. 1A, $n = 8$).[36,37] At 2 weeks after tooth extraction, all control nondiabetic *db/+* mice without Zol treatment underwent complete socket wound healing with mucosal coverage and normal bone formation; histologically, the void socket was regenerated with woven alveolar bone and epithelial migration (Fig. 1B, upper panels). However, 37.5% (3 of 8) of *db/db* mice without Zol treatment clinically exhibited open socket with delayed mucosal coverage, but bone healing was proceeding with normal woven bone pattern as in controls (Fig. 1C, upper panels, and Fig. 1D). On the other hand, 75% (6 of 8) of *db/db* mice treated with Zol developed BRONJ-like lesions at 2 weeks after tooth extraction, clinically manifested as open extraction sockets with unfilled bone defect, exposed necrotic bone, and lack of epithelial coverage (Fig. 1C, lower panels, and
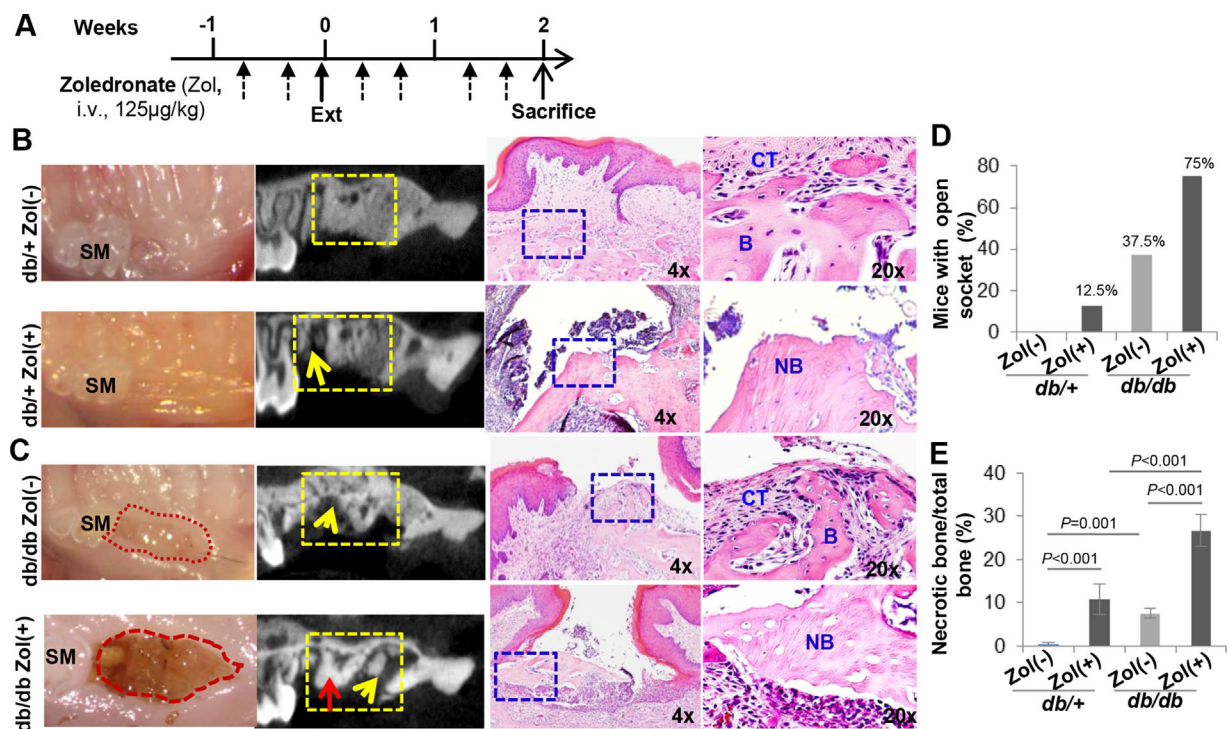
Fig. 1. Increased incidence of BRONJ-like lesions in *db/db* mice. (*A*) BRONJ induction protocol: mice were administered (iv) with two doses of zoledronate (Zol, 125 μg/kg) 1 week before tooth extraction (Ext) followed by Zol injection twice a week for 2 weeks (*n* = 8). (*B*) Background *db/+* control mice without Zol treatment, *db/+* Zol⁻, or treated with Zol, *db/+* Zol⁺. (*C*) *db/db* mice without Zol treatment, *db/db* Zol⁻, or treated with Zol, *db/db* Zol⁺. The left panel showed gross clinical appearance of gingival mucosa at the extraction sites at 2 weeks after tooth extraction. Red tracings showed the apparent mucosal disruption with exposed bone at the extracted site adjacent to the second molar (SM). The second panel is a representative micro-CT image showing necrotic bone (red arrow) and unhealed sockets (yellow arrows). The third and fourth panels are representative images of H&E staining showing connective tissues (CT), new bone formation (B), and necrotic bones (NB). Scale bars = 100 μm. (*D*) Percentage of mice with clinically open sockets (*n* = 8). (*E*) Quantification of necrotic bone areas in mice with or without Zol treatment at 2 weeks after tooth extraction. Data are presented as mean ± SD (*n* = 8). *db/db* Zol⁻ versus *db/+* Zol⁻, *p* = 0.001; *db/+* Zol⁺ versus *db/+* Zol⁻, *p* < 0.001; *db/db* Zol⁺ versus *db/db* Zol⁻, *p* < 0.001; *db/db* Zol⁺ versus *db/+* Zol⁺, *p* < 0.001.

Fig. 1*D*) compared with 12.5% (1 of 8) incidence in control *db/+* mice (Fig. 1*B*, lower panels, and Fig. 1*D*). μCT analysis of BRONJ lesions showed irregular alveolar bone ridge with socket defects and mottled trabecular pattern with mixed radiopaque/radiodense areas of necrotic bone (Fig. 1*B, C*, lower second panels). H&E staining demonstrated BRONJ-like phenotypes characterized by a lack of epithelial lining in areas of necrotic bones with empty lacunae, presence of inflammatory infiltrates, and soft tissue fibrosis (Fig. 1*B, C*, lower third and fourth second panels). Most significantly, increased zones of necrotic or dead bone existed in the unhealed sockets of Zol-treated *db/db* mice compared with treatment controls (Zol⁺, 26.72 ± 4.8149% versus Zol⁻, 7.53 ± 0.9963, *p* < 0.001; 95% confidence interval [CI] 15.7099, 22.6601; *n* = 8) (Fig. 1*E*).

We further evaluated socket wound healing in *db/db* mice at 4 weeks post-extraction (Supplemental Fig. S1*A*; *n* = 8). In *db/db* mice without Zol treatment, improved socket healing was observed with only 25% (2 of 8) mice exhibiting delayed epithelial coverage (compared with 37.5% at 2-week follow-up), whereas woven bone formation appeared normal (Supplemental Fig. S1*B, C*). However, there was still 50% (4 of 8) of *db/db* mice treated with Zol exhibiting BRONJ phenotypes with presence of bone necrosis, loose sequestra, and lack of epithelial coverage at the extraction socket sites (Supplemental Fig. S1*B, D*). Overall, Zol treatment had little effect on body weight and blood glucose

levels in *db/db* mice throughout the study (*p* > 0.05) (Supplemental Fig. S2*A, B*). These results have demonstrated an overall delayed oral mucosal wound healing and an increased incidence of BRONJ in *db/db* mice undergoing dental extraction.

Increased NLRP3 activation correlates with delayed wound healing and BRONJ-like lesions in *db/db* mice

To explore the correlation between NLRP3 inflammasome activation and BRONJ development, we initially examined the expression of NLRP3 inflammasome components at the local socket wound sites. Immunohistochemical studies showed that the sockets of BRONJ *db/db* mice constitutively expressed a higher level of NLRP3, caspase-1, and IL-1β protein than nondiabetic *db/+* mice (NLRP3: *db/db* BRONJ⁻, 18.424 ± 2.7421% versus *db/+* BRONJ⁻, 4.012 ± 1.1167%; *p* < 0.001; 95% CI 8.1282, 20.6958; caspase-1: *db/db* BRONJ⁻, 19.506 ± 3.0402% versus *db/+* BRONJ⁻, 4.42 ± 0.8467%; *p* < 0.001, 95% CI 9.5356, 20.6343; IL-1β: *db/db* BRONJ⁻, 15.27 ± 3.2213% versus *db/+* BRONJ⁻, 4.426 ± 1.2977%; *p* = 0.002, 95% CI 3.8577, 17.8303; *n* = 5) (Fig. 2*A–F*). Meanwhile, the local expression of these inflammasome components at the socket sites of BRONJ *db/db* mice was significantly increased compared with BRONJ controls (NLRP3: *db/db* BRONJ⁺, 33.896 ± 5.6596% versus *db/db* BRONJ⁻, 18.424 ± 2.7421%; *p* < 0.001, 95% CI 9.1882, 21.7558; caspase-1: *db/db* BRONJ⁺, 35.032 ± 4.9793% versus *db/db* BRONJ⁻, 19.506 ± 3.0402%;
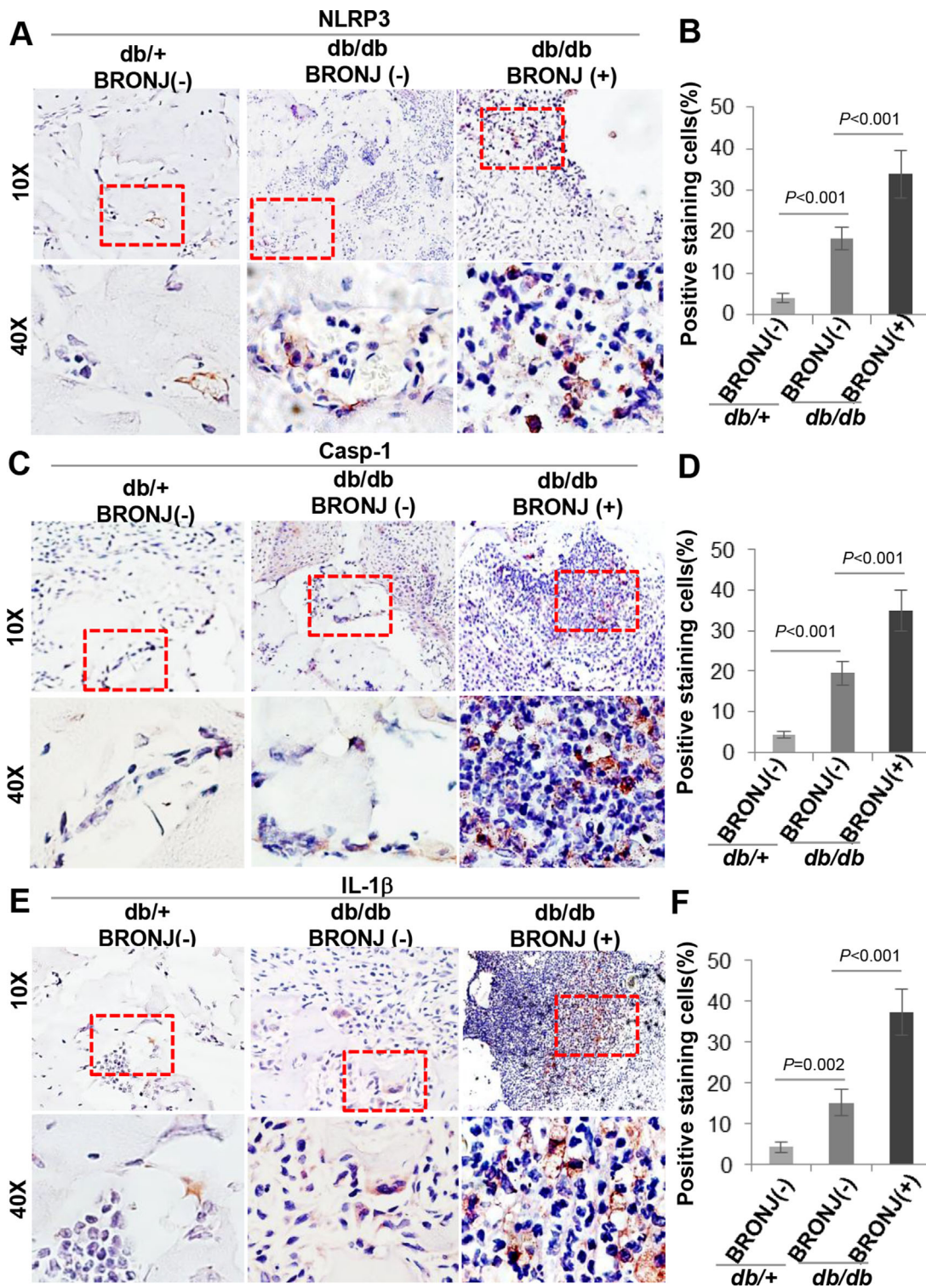
Fig. 2. Increased NLRP3 activation in BRONJ-like lesions in *db/db* mice. Paraffin-embedded sections of oral socket tissues from *db/db* mice with or without BRONJ were immunostained for NLRP3 (*A, B*), caspase-1 (*C, D*), and IL-1β (*E, F*), whereas socket tissues from *db/+* mice without BRONJ were used as controls. Positive cells were counted in six randomly selected high-power fields and averaged. Scale bars = 50 μm. *db/+* BRONJ⁻, *db/+* mice without BRONJ; *db/db* BRONJ⁻, *db/db* mice without BRONJ; *db/db* BRONJ⁺, *db/db* mice with BRONJ. Data are presented as mean ± SD (*n* = 5). For NLRP3 and caspase-1 expression (*B, D*), *db/db* BRONJ⁻ versus *db/+* BRONJ⁻, *db/db* BRONJ⁺ versus *db/db* BRONJ⁻, $p < 0.001$. For IL-1β expression (*F*), *db/db* BRONJ⁻ versus *db/+* BRONJ⁻, $p = 0.002$; *db/db* BRONJ⁺ versus *db/db* BRONJ⁻, $p < 0.001$.

$p < 0.001$, 95% CI 9.9756, 21.0764; IL-1β: db/db BRONJ$^+$, 37.482 ± 5.6072% versus db/db BRONJ$^-$, 15.27 ± 3.2213%; $p < 0.001$, 95% CI 15.2257, 29.1983; $n = 5$) (Fig. 2A–F). Immunofluorescence staining showed that the increased expression of NLRP3, caspase-1, and IL-1β protein was located primarily in F4/80$^+$ macrophages (Supplemental Fig. S3), suggesting that NLRP3 activation in macrophages may play an important role in BRONJ development in db/db mice.

We then explored the effect of Zol administration on NLRP3 inflammasome activation in BMDMs, and demonstrated that BMDMs derived from db/db mice constitutively secrete a relatively high level of IL-1β compared with those from $db/+$ mice (db/db, 48.875 ± 8.6987 pg/mL versus $db/+$, 16.65 ± 6.3271 pg/mL, $p = 0.045$; 95% CI 0.2995, 64.7396; $n = 3$) (Fig. 3A). In response to LPS/nigericin (NG) stimulation, db/db BMDMs exhibited a 1.77-fold increase in the secretion of IL-1β in contrast to $db/+$ BMDMs (db/db, 197.56 ± 18.1189 pg/mL versus $db/+$, 111.58 ± 15.8075 pg/mL; $p < 0.001$; 95% CI 53.4625, 118.4989; $n = 3$) (Fig. 3A). Treatment with Zol further increased LPS/nigericin (NG)-stimulated IL-1β secretion by 1.63- and 1.86-fold in db/db BMDMs (LPS/NG Zol$^+$, 322.59 ± 28.4248 pg/mL versus LPS/NG Zol$^-$, 197.56 ± 18.1189 pg/mL, $p < 0.001$; 95% CI 92.5085, 157.5449; $n = 3$) and $db/+$ BMDMs (LPS/NG Zol$^+$, 207.12 ± 11.8664 pg/mL versus LPS/NG Zol$^-$, 111.58 ± 15.8075 pg/mL; $p < 0.001$; 95% CI 63.0191, 128.0555; $n = 3$), respectively (Fig. 3B, E). The net secretion of IL-1β induced by Zol was significantly higher in db/db BMDMs compared with $db/+$ BMDMs (db/db, 322.59 ± 28.4248 pg/mL versus $db/+$, 207.12 ± 11.8664 pg/mL; $p < 0.001$; 95% CI 82.9518, 147.9882; $n = 3$) (Fig. 3B, E). Similarly, Zol treatment led to 1.66- and 1.52-fold increase in the

expression of LPS/nigericin (NG)-induced cleaved caspase-1 in $db/+$ BMDMs ($p = 0.001$) (Fig. 3C, D) and db/db BMDMs ($p < 0.001$) (Fig. 3F, G), respectively. These results suggest that db/db BMDMs displayed increased responses to NLRP3 activators and Zol stimulation, thus further correlating the upregulation of NLRP3 activation with healed socket wounds in Zol-treated diabetic mice.

Additionally, we analyzed the serum levels of IL-1β and IL-17 in both $db/+$ and db/db mice at 2 weeks after tooth extraction. Our results showed that db/db mice had a higher basal serum level of IL-1β (db/db, 61.185 ± 11.6022 pg/mL versus $db/+$, 36.54 ± 5.1465 pg/mL; $p = 0.019$; 95% CI 3.7608, 45.5292; n = 4) and IL-17 (db/db, 346.4267 ± 50.5386 pg/mL versus $db/+$, 37.367 ± 4.8865 pg/mL; $p < 0.001$; 95% CI 233.412, 384.728; n = 4) compared with that of diabetic $db/+$ mice (Supplemental Fig. S2C, D). Furthermore, Zol treatment increased the serum levels of IL-1β (Zol$^+$, 124.693 ± 14.1033 pg/mL versus Zol$^-$, 61.185 ± 11.6022 pg/mL; $p < 0.001$; 95% CI 42.6238, 84.3922) and IL-17 (Zol$^+$, 515.594 ± 26.9574 pg/mL versus Zol$^-$, 346.4267 ± 50.5386 pg/mL; $p < 0.001$; 95% CI 93.499, 244.815) in db/db mice (Supplemental Fig. S2C, D), whereas tooth extraction alone had no effects on serum levels of IL-1β and IL-17 in both $db/+$ and db/db mice ($p > 0.05$; n = 4) (Supplemental Fig. S2E, F).

Blocking NLRP3 activation promotes extraction socket healing and inhibits BRONJ development in db/db mice

We next examined the effects of blocking NLRP3 inflammasome on delayed oral socket wound healing and BRONJ formation in db/db mice. As expected, treatment with Ac-YVAD-cmk, a
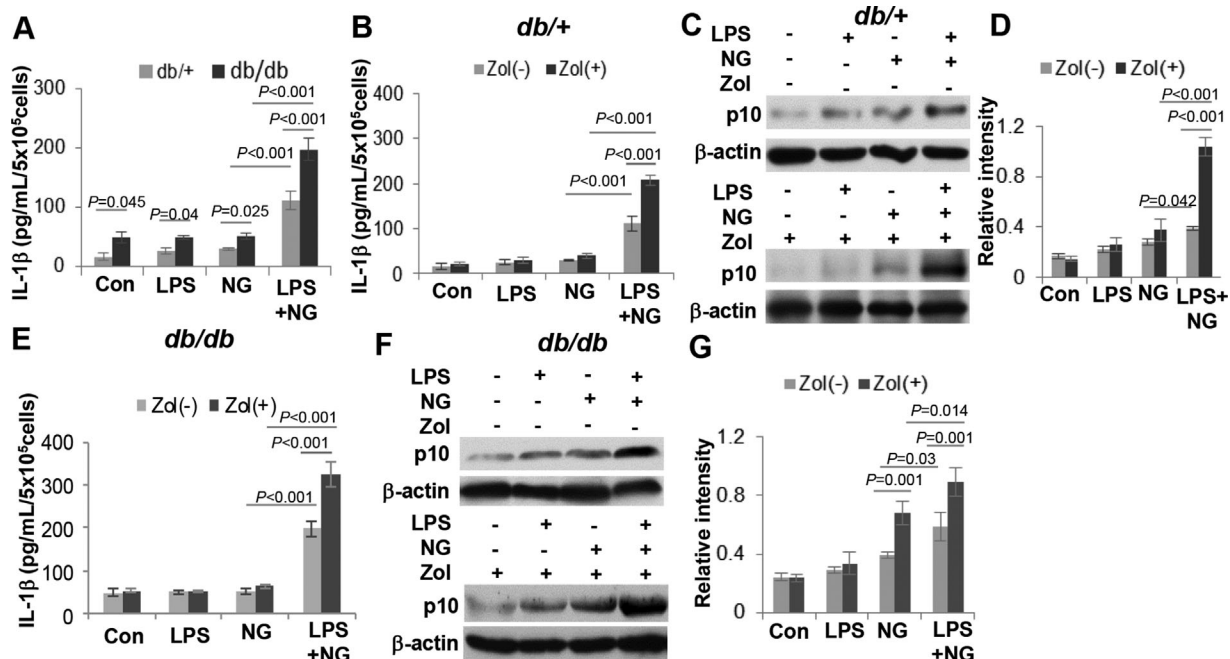
Fig. 3. Zol treatment enhanced NLRP3 activation in BMDMs. BMDMs were cultured in the presence of 10 ng/mL of M-CSF for 7 days, followed by priming with 200 ng/mL of lipopolysaccharide (LPS) for 3 hours and then stimulated with 20 μM nigericin (NG) for 30 minutes. The secretion levels of IL-1β in the supernatants and the expression of cleaved caspase-1 were determined by ELISA and Western blot, respectively. Data are presented as mean ± SD (n = 3). (A) db/db BMDMs secreted relatively high basal level of IL-1β compared with diabetic $db/+$ BMDMs; $p = 0.045$. In response to LPS/NG, db/db BMDMs secreted 1.77-fold of IL-1β above $db/+$ BMDMs; $p < 0.001$. (B–D) Zol treatment led to a 1.86- and 1.66-fold increase in LPS/NG-stimulated IL-1β secretion (B) and cleaved caspase-1 expression (C, D), respectively, in $db/+$ BMDMs; $p < 0.001$. (E–G) Zol treatment led to a 1.63- and 1.52-fold increase in LPS/NG-stimulated IL-1β secretion (E) and cleaved caspase-1 expression (F, G), respectively, in db/db BMDMs; $p < 0.001$.

specific inhibitor of caspase-1 activity, or glyburide, an antidiabetic drug and recognized NLRP3 inhibitor,[40] significantly decreased the body weight ($p < 0.01$; $n = 10$) (Supplemental Fig. S4A). Treatment with glyburide significantly reduced blood glucose concentration in *db/db* mice (glyburide, 715.00 ± 99.5188 mg/dL versus control, 845.88 ± 81.1723 mg/dL, $p = 0.012$; $n = 10$), whereas caspase-1 inhibition showed a moderate effect (Ac-YVAD-cmk, 750.62 ± 62.65 mg/dL versus control, 845.88 ± 81.17 mg/dL, $p = 0.076$; $n = 10$) (Supplemental Fig. S4B). Notably, treatment with either Ac-YVAD-cmk or glyburide markedly promoted mucosal healing and woven bone formation in Zol-treated *db/db* mice (Fig. 4A, B), whereas the improvement of delayed socket wound healing correlated with a decrease in serum levels of IL-1β (control, 74.7233 ± 6.2625 pg/mL versus Ac-YVAD-cmk, 38.5333 ± 5.6022 pg/mL, $p = 0.004$, 95% CI 11.2991, 61.0809; control, 74.7233 ± 6.2625 pg/mL versus glyburide, 39.4633 ± 6.9829 pg/mL, $p = 0.005$, 95% CI 10.3691, 60.1509; $n = 3$) (Fig. 4C). Moreover, our results showed that treatment with these inhibitors markedly decreased the incidence of BRONJ and attenuated disease severity in *db/db* mice (Fig. 4D–F), which was also accompanied by a decrease in serum level of IL-1β (Zol^+, 137.19 ± 13.6267 pg/mL versus Zol^+/Ac-YVAD-cmk, 56.8967 ± 7.9071 pg/mL, $p < 0.001$; 95% CI 55.4024, 105.1842; Zol^+, 137.19 ± 13.6267 pg/mL versus Zol^+/glyburide, 62.1867 ± 11.2538 pg/mL, $p < 0.001$; 95% CI 50.1124, 99.8942; $n = 3$) (Fig. 4G). To further demonstrate the contributory role of NLRP3 in BRONJ pathogenesis, we exposed *Nlrp3*^{-/-} mice to Zol treatment followed by tooth extraction and found that none of these mice developed clinical BRONJ-like phenotype at 2 weeks postoperatively ($n = 10$) (Fig. 5A), compared with a 10% to 20% incidence of BRONJ observed in wild-type C57BL/6 mice (Fig. 1D). [37] Histological examination showed complete epithelial migration and woven bone formation in both Zol-treated and treated *Nlrp3*^{-/-} mice (Fig. 5A). Meanwhile, systemic administration of Zol did not affect the serum level of IL-1β (Fig. 5B) and showed no obvious effects on NLRP3 activator-mediated secretion of IL-1β by BMDMs derived from *Nlrp3*^{-/-} mice (Fig. 5C). These compelling findings support the notion that NLRP3 activation plays an important role in impaired oral socket wound healing and the increased incidence of BRONJ in diabetic mice.

Zol treatment augmented IL-1 β secretion in macrophages

Next, we determined the effect of Zol treatment on NLRP3-dependent IL-1β secretion in macrophages. We first demonstrated that Zol treatment resulted in approximately 1.5-fold increase in nigericin (NG)-induced IL-1β secretion by LPS-primed murine J774.A1 macrophages (LPS/NG+Zol 1μM, 830.356 ± 56.4225 pg/mL versus LPS/NG, 566.035 ± 52.1036 pg/mL, $p < 0.001$, 95% CI 153.5691, 375.0709; LPS/NG+Zol 5μM, 921.431 ± 83.4758 pg/mL versus LPS/NG, 566.035 ± 52.1036 pg/mL, $p < 0.001$, 95% CI 244.6291, 466.1309; $n = 3$) (Fig. 6A). Correspondingly, we also showed that Zol treatment further increased LPS/NG-induced expression of cleaved casase-1 in J774A.1 cells (Fig. 6B). Similarly, treatment with 5 μM Zol led to a 1.76-fold increase in IL-1β secretion in LPS-primed J774A.1 cells when stimulated with ATP as the second signal (LPS/ATP+Zol 5 μM, 464.661 ± 44.0398 pg/mL versus LPS/ATP, 263.584 ± 28.4477 pg/mL, $p < 0.001$, 95% CI 112.7729, 289.3811; $n = 3$) (Fig. 6C). As expected, stimulation of LPS-primed J774A.1 macrophages with nigericin had no obvious effects on the secretion of TNF-α, an NLRP3-independent cytokine (LPS,

565.8 ± 52.2549 pg/mL versus LPS/NG, 560.47 ± 24.3531 pg/mL, $p = 1.000$; $n = 3$); likewise, Zol effect is specifically NLRP3 dependent and showed no obvious effects on LPS-induced TNF-α secretion (LPS/Zol, 623.21 ± 19.5615 pg/mL versus LPS, 565.8 ± 52.2549 pg/mL, $p = 0.449$; $n = 3$) (Supplemental Fig. S5A). Moreover, we showed that BMDMs derived from *Nlrp3*^{-/-} mice failed to secrete IL-1β in response to LPS/nigericin (NG) stimulation and that Zol treatment did not affect IL-1β secretion in *Nlrp3*^{-/-} BMDMs (Supplemental Fig. S5B).

We further tested the effect of Zol treatment on NLRP3-dependent IL-1β secretion in human THP-1 monocytes. THP-1 monocytes were differentiated with 100 ng/mL PMA for 3 hours as the first signal, followed by stimulation with 5 mM ATP as the second signal. Our results showed that treatment with 5 μM Zol led to a 1.45-fold increase in ATP-induced IL-1β secretion in PMA-differentiated THP-1 macrophages (ATP/Zol 5 μM, 566.866 ± 35.3882 pg/mL versus ATP, 391.42 ± 28.6299 pg/mL, $p < 0.001$, 95% CI 107.6874, 243.2046; $n = 3$) (Fig. 6D). Accordingly, treatment with 5 μM Zol further increased the expression of cleaved caspase-1 in PMA-differentiated THP-1 macrophages in response to ATP stimulation (Fig. 6D). Similarly, treatment with 5 μM Zol increased IL-1β secretion by 1.74-fold in LPS-primed undifferentiated THP-1 monocytes that were subsequently stimulated by nigericin (NG) (LPS/NG+Zol 5 μM, 136.49 ± 9.8879 pg/mL versus LPS/NG, 78.582 ± 5.8452 pg/mL, $p < 0.001$, 95% CI 34.8379, 80.7955; $n = 3$) (Fig. 6E). Altogether, these results suggest that Zol treatment enhances IL-1β secretion in both murine and human monocytes/macrophages in an NLRP3-dependent pathway.

## Mechanisms of Zol induced NLRP3 activation in macrophages

Next, we determined whether addition of farnesyl pyrophosphate (FPP) and geranylgeranyl pyrophosphate (GGPP), the intermediate metabolites of the mevalonate pathway,[41] could reverse Zol-mediated effect on IL-1β secretion. We showed that supplementation with GGPP could slightly decrease LPS/nigericin (NG)-induced IL-1β secretion (LPS/NG, 596.1573 ± 15.8182 pg/mL versus LPS/NG+GGPP, 503.897 ± 22.33 pg/mL; $p = 0.045$, $n = 3$), whereas FPP had no obvious effect (LPS/NG, 596.1573 ± 15.8182 pg/mL versus LPS/NG+FPP, 567.1163 ± 24.2186 pg/mL; $p = 0.905$, $n = 3$) (Fig. 7A, B). However, a combined addition of FPP and GGPP almost completely abolished Zol-enhanced IL-1β release from LPS/NG-activated macrophages (LPS/NG+Zol, 1050.643 ± 76.2014 pg/mL versus LPS/NG+Zol+FPP, 478.663 ± 13.3641 pg/mL; LPS/NG+Zol, 1050.643 ± 76.2014 pg/mL versus LPS/NG+Zol+GGPP, 650.8403 ± 29.4136 pg/mL; $p < 0.001$, $n = 3$) (Fig. 7A, B); these findings suggest that the depletion of prenyl pyrophosphates in macrophages is indispensable for Zol-enhanced NLRP3 activation and consequential release of bioactive IL-1β.

We next pretreated J774.A1 macrophages with glyburide, an ATP-dependent K$^+$ channel blocker and NLRP3 inhibitor, or Ac-AVYD-CMK, a specific inhibitor of caspase-1 activity, followed by treatment with Zol and subsequent stimulation with LPS/NG. We showed that treatment with Ac-AVYD-CMK and glyburide (GL) not only significantly suppressed LPS/NG-induced IL-1β release (LPS/NG, 802.9962 ± 125.7601 pg/mL versus LPS/NG+Ac-YVAD-CMK, 192.383 ± 31.044 pg/mL; LPS/NG, 802.9962 ± 125.7601 pg/mL versus LPS/NG+GL, 330.575 ± 36.0632 pg/mL; $p < .001$; $n = 3$) but also abrogated Zol-enhanced IL-1β release in response to LPS/NG stimulation (LPS/NG+Zol, 1291.581 ± 168.893 pg/mL versus LPS/NG+Zol+Ac-YVAD-CMK, 470.706 ± 38.9915 pg/mL;
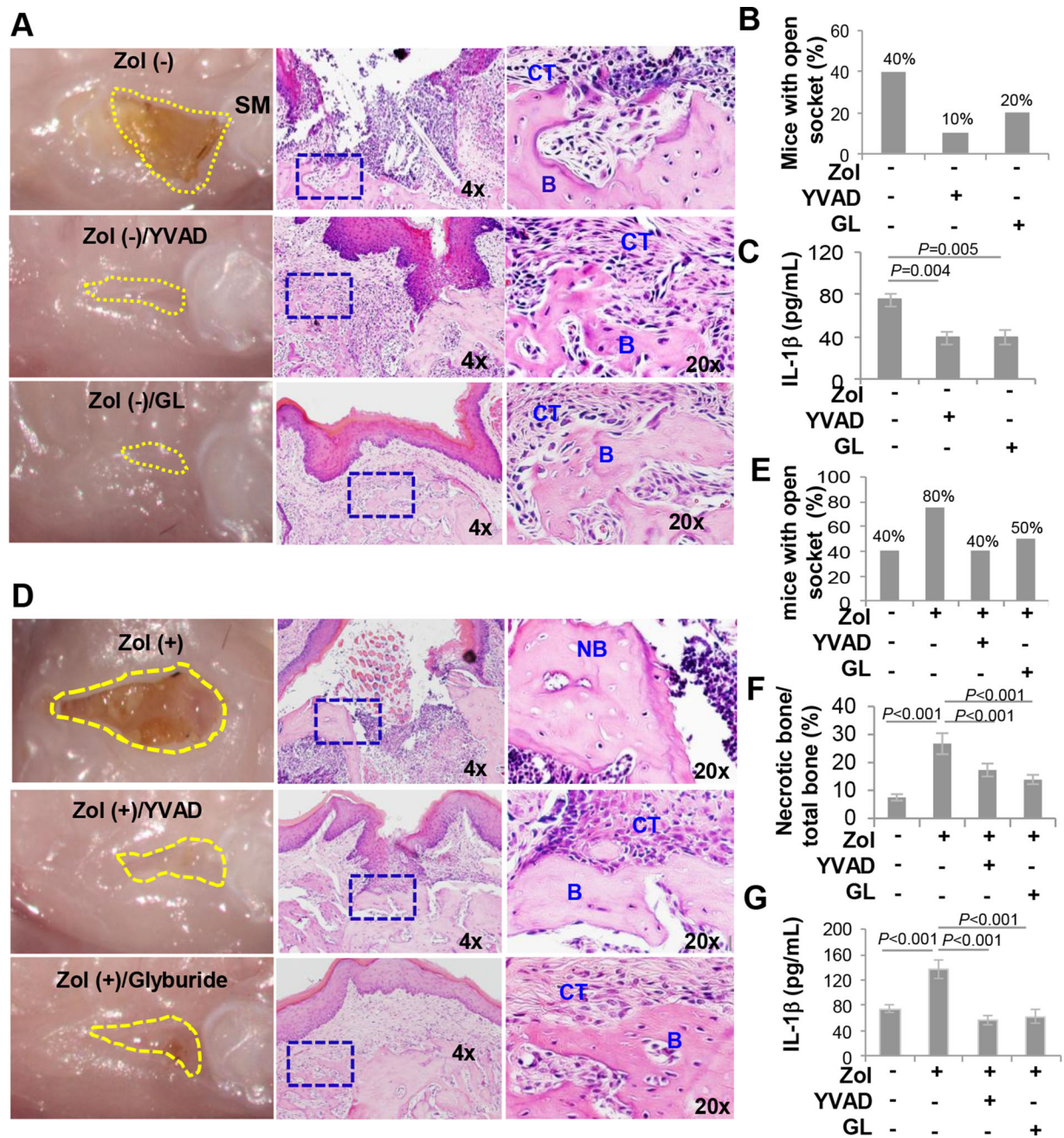
Fig. 4. Blocking NLRP3 inflammasome activity in vivo promotes oral socket wound healing in *db/db* mice. (*A*) After tooth extraction, *db/db* mice without Zol treatment were intraperitoneally injected with either Ac-YVAD-cmk, a specific caspapse-1 inhibitor (5 mg/kg, twice a week), Zol⁻/YVAD, or glyburide (GL) (50 mg/kg, once per day), Zol⁻/GL, for 2 weeks (*n* = 10). Oral socket tissues were collected and gross clinical appearances were photographed, sectioned, and stained with H&E. Scale bars = 100 m. CT = connective tissue; B = newly formed bone. (*B*) Percentage of *db/db* mice with unhealed open sockets (*n* = 10). (*C*) Serum IL-1β levels as determined by ELISA. Data are presented as mean ± SD (*n* = 3). Zol⁻ versus Zol⁻/YVAD, *p* = 0.004; Zol⁻ versus Zol⁻/GL, *p* = 0.005. (*D*) After tooth extraction, *db/db* mice with Zol treatment were intraperitoneally injected with either Ac-YVAD-cmk, a specific caspase-1 inhibitor (5 mg/kg, twice a week), Zol⁺/YVAD, or glyburide (GL) (50 mg/kg, once per day), Zol⁺/GL, for 2 weeks. Oral socket tissues were collected and gross clinical appearances were photographed, sectioned, and stained with H&E staining. Scale bar = 100 μm. CT = connective tissue; B = newly formed bone; NB = necrotic bones. (*E*) Percentage of *db/db* mice with unhealed open sockets (*n* = 10). (*F*) Quantification of necrotic bone of oral socket wound of *db/db* mice with different treatment. Data are presented as mean ± SD (*n* = 10). Zol⁺ versus Zol⁻, Zol⁺ versus Zol⁺/YVAD, Zol⁺ versus Zol⁺/GL, *p* < 0.001. (*G*) Serum IL-1β levels as determined by ELISA. Data are presented as mean ± SD (*n* = 3). Zol⁺ versus Zol⁻, Zol⁺ versus Zol⁺/YVAD, Zol⁺ versus Zol⁺/GL, *p* < 0.001.
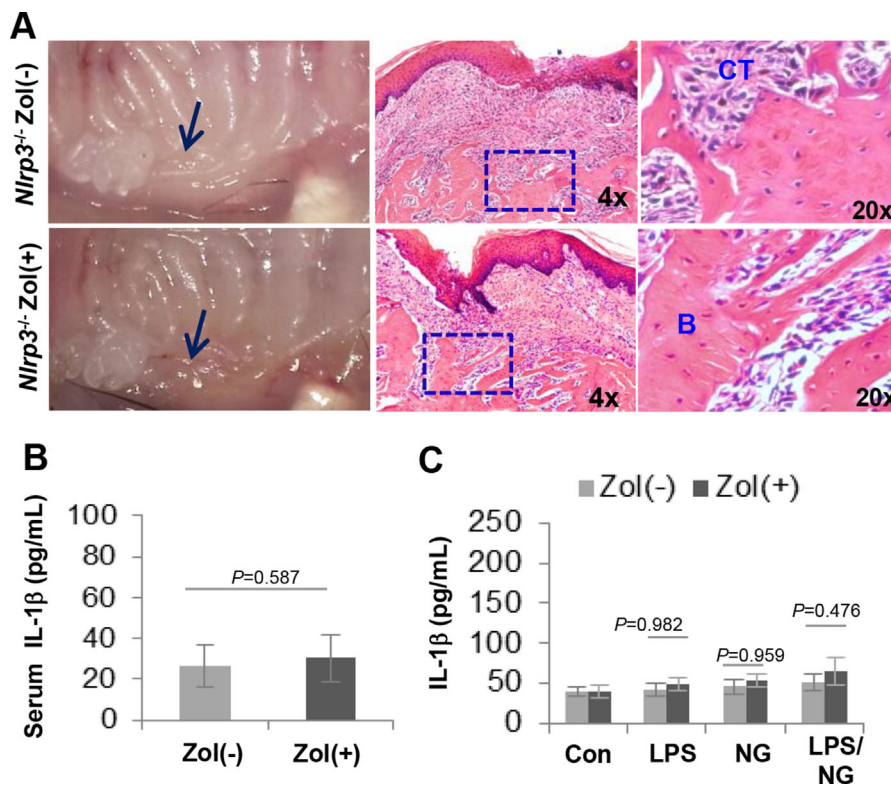
Fig. 5. *Nlrp3*^{-/-} mice do not develop BRONJ after Zol treatment. *Nlrp3*^{-/-} mice were intravenously administered with two doses of zoledronate (Zol, 125 μg/kg) 1 week before tooth extraction (Ext) followed by Zol injection twice a week for 2 weeks (n = 10), *Nlrp3*^{-/-} Zol[+]; *Nlrp3*^{-/-} mice without Zol treatment were used as controls, *Nlrp3*^{-/-} Zol[-]. (A) The left panel showed gross clinical appearance of gingival mucosa at the extraction sites at 2 weeks after tooth extraction. Arrows pointed to the extracted site, showing complete mucosal healing. The second and third panels are representative images of H&E staining showing connective tissues (CT) and new bone formation (B). (B) In vivo administration of Zol had no obvious effects on serum levels of IL-1β of *Nlrp3*^{-/-} mice. Zol[+] versus Zol[-], p = 0.587. (C) In vivo administration of Zol showed no obvious effects on LPS/NG-induced IL-1β release by bone marrow-derived macrophages (BMDMs) from *Nlrp3*^{-/-} mice. BMDMs were primed with 200 ng/mL LPS for 4 hours followed by stimulation with 20 μM NG. The secretion level of IL-1β in the supernatants was determined by ELISA (n = 3). LPS/NG Zol[+] versus LPS/NG Zol[-], p = 0.476.

LPS/NG+Zol, 1291.581 ± 168.893 pg/mL versus LPS/NG+Zol+ GL, 210.414 ± 28.9106 pg/mL; $p < 0.001$; n = 3) (Fig. 7C, D).

To determine whether $P2X_7$ receptor-gated ion channels, endogenous reactive oxygen species (ROS), and cathepsin B release play a role in NLRP3 inflammasome activation,[32,39] J774.A1 cells were pretreated with either A438079, an antagonist for $P2X_7R$, or *N*-acetyl-cysteine (NAC), a scavenger of reactive oxygen species, or CA-074-Me, an inhibitor of Cathepsin B release, followed by treatment with Zol and subsequent LPS/NG stimulation. Our results indicated that treatment with A438079 and NAC significantly abrogated Zol-enhanced IL-1β release in response to LPS/NG stimulation (LPS/NG+Zol, 1291.581 ± 168.893 pg/mL versus LPS/ NG+Zol+A438079, 110.298 ± 16.6137 pg/mL; LPS/NG+Zol, 1291.581 ± 168.893 pg/mL versus LPS/NG+Zol+NAC, 155.162 ± 19.9631 pg/mL; $p < 0.001$, n = 3) (Fig. 7E, F), but inhibition of cathepsin B by CA-074-Me had no obvious effects on Zol-induced IL-1β secretion (LPS/NG+Zol, 1291.581 ± 168.893 pg/mL versus LPS/NG+Zol+CA-074-Me, 1137.776 ± 231.9006 pg/mL; $p = 0.549$, n = 3) (Supplemental Fig. S5C), suggesting that lysosome disruption was not part of the Zol-induced NLRP3 activation cascade. These experiments further confirm that Zol-mediated activation of IL-1β secretion in monocytes/macrophages is dependent on the canonical NLRP3 inflammasome pathway; further studies are needed to delineate its underlying mechanism.

Discussion

The cellular and molecular mechanisms underlying diabetes-associated delayed skin wound healing have been extensively explored,[20–23] but much remains to be explored on problematic wounds of the oral cavity, particularly BRONJ, in poorly controlled diabetes. In the present study, we demonstrated that diabetic *db/db* mice exhibited a significantly increased incidence and severity of BRONJ-like disease, which is closely correlated with elevated NLRP3 activation in macrophages at the local lesions. Our in vitro data indicated that *db/db* BMDMs secreted higher levels of IL-1β compared with nondiabetic *db/+* BMDMs in response to NLRP3 inducers, whereas NLRP3-dependent IL-1β release was further enhanced by zoledronate treatment. Importantly, blockade of NLRP3 activity in vivo markedly improves delayed socket healing and decreases the incidence of BRONJ-like disease in diabetic mice. These results support the hypothesis that upregulation of NLRP3 activation in macrophages may play an important role in BRONJ development.

Most recently, the new term "medication-related osteonecrosis of the jaw" (MRONJ) has been introduced to replace the nomenclature "bisphosphonate-related osteonecrosis of the jaw" (BRONJ) to reflect the growing number of ONJ cases associated with other antiresorptive (denosumab) and anti-angiogenic
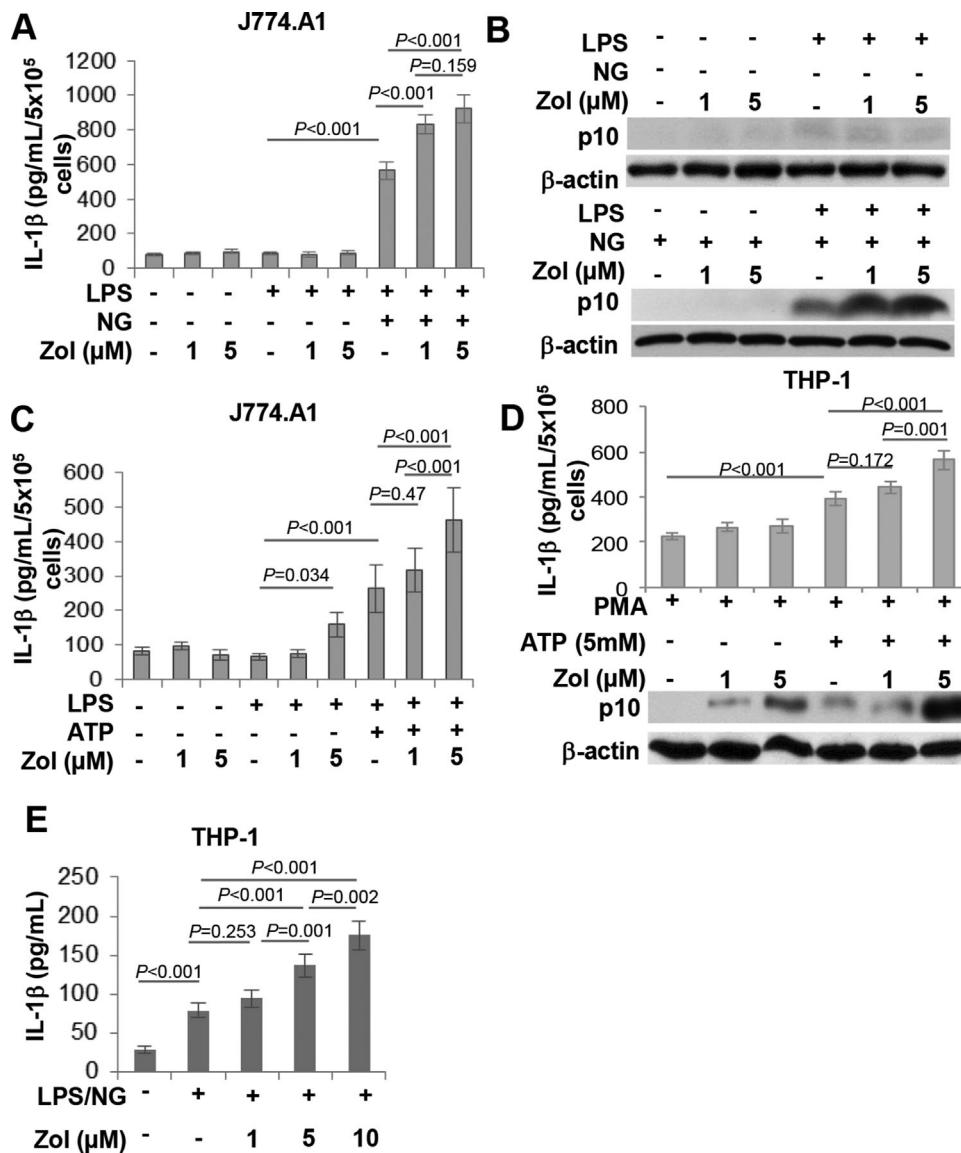
Fig. 6. Zol treatment augments NLRP3 inflammasome activation in mice and human macrophages. (*A, B*) Murine J774A.1 macrophages were cultured in the presence of 1 and 5 μM Zol for 24 hours, followed by priming with 200 ng/mL of LPS for 4 hours and then stimulating with 20 μM nigericin (NG) for 30 minutes. The secretion of IL-1β and expression of cleaved caspase-1 (p10) were determined by ELISA (*A*) and Western blot (*B*), respectively (*n* = 3). Treatment with Zol increased LPS/NG-stimulated IL-1β secretion by ~1.5-fold, *p* < 0.001. Data are presented as mean ± SD. (*C*) J774A.1 macrophages were cultured in the presence of 1 and 5 μM Zol for 24 hours, followed by priming with 200 ng/mL of LPS for 4 hours and then stimulating with 5 mM ATP for 30 minutes. The secretion of IL-1β was determined by ELISA. Treatment with 5 μM of Zol led to a 1.76-fold increase in LPS/ATP-stimulated IL-1β secretion, *p* < 0.001. (*D*) PMA-differentiated THP-1 macrophages were cultured in the presence of 1 and 5 μM Zol for 24 hours, followed by stimulating with 5 mM ATP for 30 minutes. The secretion of IL-1β in the supernatants and the expression of cleaved caspase-1 were determined by ELISA (upper panel) and Western blot (lower panel), respectively. Treatment with 5 μM of Zol led to a 1.45-fold increase in ATP-induced IL-1β secretion, *p* < 0.001. Data are presented as mean ± SD. (*E*) Human THP-1 monocytes were cultured in the presence of different concentrations of Zol for 24 hours, and then primed with LPS (200 ng/mL) for 4 hours followed by stimulation with 20 μM nigericin (LPS/NG) for 30 minutes. The secretion levels of IL-1β in supernatants were determined by ELISA. LPS/NG+Zol (5 μM) versus LPS/NG, *p* < 0.001; LPS/NG+Zol (10 μM) versus LPS/NG, *p* < 0.001. Data are presented as mean ± SD.

therapies.[42] Even though clinical application of both bisphosphonates and denosumab causes similar incidence of ONJ, they have distinct biodistribution and pharmacologic dynamics and functions.[1] Bisphosphonates exert their irreversible antiresorptive effects long after their administration because of their incorporation and accumulation in the bone mineral.[43] On the contrary, the antiresorptive effect of denosumab is rapidly reversible

because it does not need to incorporate in bone mineral to exert its anti-osteoclastic function.[44,45] Most recently, de Molon and colleagues have demonstrated that discontinuation of OPG-Fc, a specific inhibitor of RANKL, reversed the features of osteonecrosis in ONJ mice models, but discontinuation of zoledronic acid did not.[46] In the present study, we showed that 37.5% and 25% of *db/db* mice without Zol treatment exhibited a delayed oral mucosal
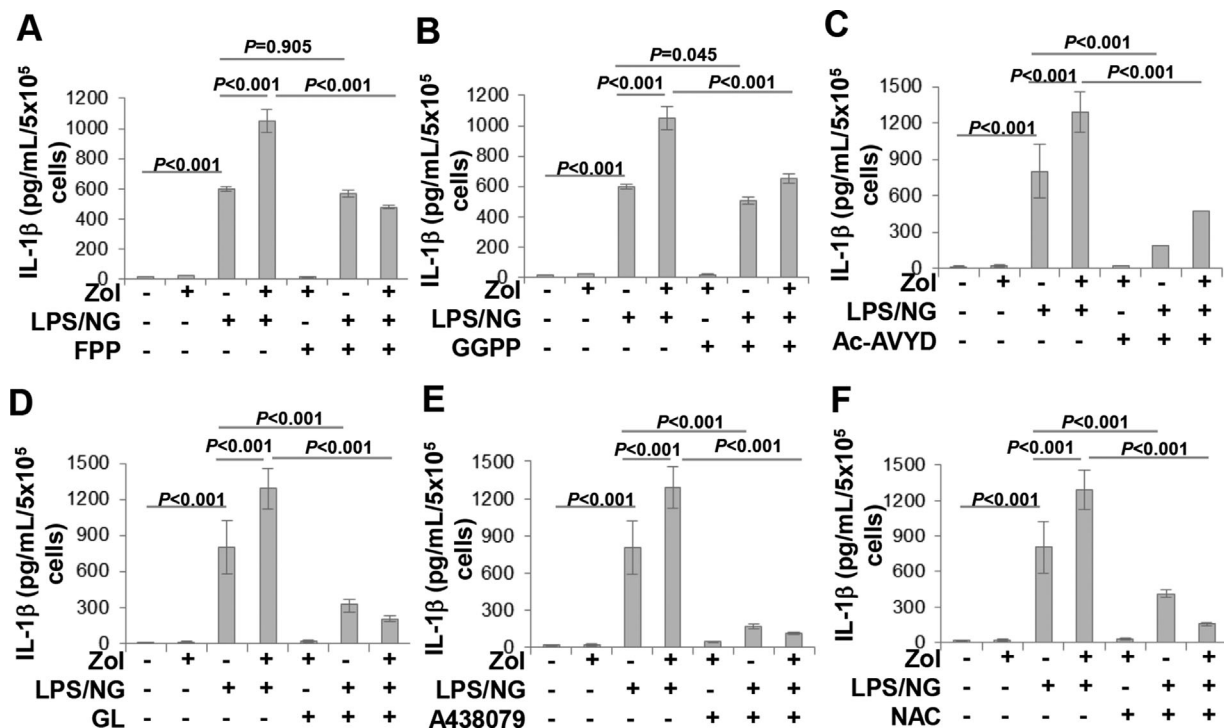
Fig. 7. Mechanisms underlying Zol-enhanced NLRP3 activation in macrophages. (*A, B*) J774A.1 macrophages were cultured in the presence of 5 μM Zol, 10 μM farnesyl pyrophosphate (FPP), or geranylgeranyl pyrophosphate (GGPP) for 24 hours followed by priming with 200 ng/mL LPS for 4 hours and stimulation with 20 μM nigericin (NG) for 30 minutes. The secretion of IL-1β in the supernatants was determined by ELISA ($n < 3$). Addition of either FPP or GGPP significantly abolished Zol-enhanced IL-1β secretion induced by LPS/NG stimulation, $p < 0.001$. (*C, D*) J774A.1 macrophages were cultured in the presence of 5 μM Zol, 20 μM Ac-YVAD-cmk (YVAD), or 200 μM glyburide (GL) for 24 hours followed by priming with 200 ng/mL LPS for 4 h and stimulation with 20 μM nigericin (NG) for 30 min. The secretion of IL-1β in the supernatants was determined by ELISA ($n = 3$). Both Ac-YVAD-cmk and GL significantly abrogated Zol-enhanced IL-1β secretion induced by LPS/NG stimulation; $p < 0.001$. (*E, F*) J774A.1 macrophages were cultured in the presence of 5 μM Zol, 20 μM A438079, or 10 mM N-acetyl cysteine (NAC) for 24 hours followed by priming with 200 ng/mL LPS for 4 hours and stimulation with 20 μM NG for 30 minutes. The secretion level of IL-1β in supernatants was determined by ELISA. Both A438079 and NAC significantly abrogated Zol-enhanced IL-1β secretion induced by LPS/NG stimulation; $p < 0.001$. Data are presented as mean ± SD.

wound healing with normal woven bone formation at 2 and 4 weeks after tooth extraction, respectively, whereas Zol administration led to BRONJ development in 75% and 50% of *db/db* mice at 2 and 4 weeks after tooth extraction, respectively. These findings further support the cumulative high dose of Zol is the etiologic cause of BRONJ formation in *db/db* mice undergoing dental extraction. However, further studies are warranted to explore whether these BRONJ-like lesions would eventually heal in *db/db* mice model after Zol discontinuation for different time periods.

Macrophage represents a malleable type of innate immune cells that plays a critical role in the clearance of necrotic/apoptotic cells and invaded pathogens, thus leading to resolution of inflammation, tissue homeostasis, and efficient wound repair.[47,48] The innate immune response involving NLRP3 inflammasome activation is one of the first line of host defense against tissue damage and pathogen invasion.[15] NLRP3 activation leads to the cleavage of pro-caspase-1 and the subsequent release of mature IL-1β.[16] In turn, NLRP3-dependent secretion of IL-1β induces a pro-inflammatory phenotype of macrophages[24,49] and also amplifies Th1 and Th17 responses,[50–52] thus constituting a positive feedback loop that bridges innate and adaptive immune responses. A growing body of evidence has shown that sustained inflammation

mediated by activation of the NLRP3 inflammasome cascade plays a critical role in the pathophysiology of numerous metabolic and inflammatory diseases, such as obesity, insulin resistance, and diabetes.[15,16] Recent studies have shown that monocytes/macrophages from diabetic patients and mice exhibit a proinflammatory phenotype[20,21,24] and a sustained NLRP3 inflammasome activation in macrophages contributes to diabetes-associated impaired skin wound healing, whereas blocking IL-1β induces a wound healing macrophage phenotype and improves wounded skin repair in type 2 diabetes.[22,23] In our current study, we have also demonstrated a constitutive elevation of NLRP3 activity in macrophages from *db/db* mice, and blocking NLRP3 activity promotes delayed socket healing in diabetic mice. These findings further support a critical role of sustained activation of the NLRP3 inflammasome cascade in diabetes-associated impairment of oral and skin wound healing.

The mevalonate metabolic pathway provides isoprenoid building blocks for the biosynthesis of vital cellular products such as prenyl pyrophosphates for posttranslational prenylation of numerous proteins.[53] Mevalonate kinase deficiency (MKD), an autosomal recessive disease caused by a genetic defect in the mevalonate pathway and isoprenoid biosynthesis, is characterized by autoinflammatory symptoms associated with increased caspase-1 activity and IL-1β overproduction.[30] Recent studies

showed that bisphosphonates and statins, inhibitors of HMG-CoA reductase, a rate-limiting enzyme of mevalonate pathway, synergized with LPS to enhance NLRP3-dependent IL-1β release in monocytes owing to defective biosynthesis of isoprenoid intermediates,[32–35] thus promoting pulmonary fibrosis and the onset of collagen type II-induced arthritis in mice.[31,54] Our data showed that Zol-enhanced NLRP3 activation in both human and mice monocytes/macrophages and Zol-mediated effects on NLRP3 activation were abrogated by the supplementation of farnesyl pyrophosphate and geranylgeranyl pyrophosphate, suggesting that depletion of farnesyl pyrophosphate and geranylgeranyl pyrophosphate was essential in Zol-induced upregulation of NLRP3 activation in macrophages. In addition, we demonstrated that BMDMs derived from Zol-treated mice showed significantly increased IL-1β release in reponse to NLRP3 activation. More importantly, our data indicated that in vivo inhibition of NLRP3 inflammmasome activity by treatment with a specific caspase-1 inhibitor and glyburide, a commonly used sulfonylurea drug for the treatment of type 2 diabetes and NLRP3 inhibitor,[40] markedly decreased the incidence and severity of BRONJ manifestation in *db/db* mice. In addition, none of the *Nlrp3*-/- mice undergoing dental extraction developed typical BRONJ-like phenotypes during the course of Zol treatment. Taken together, these findings supported our hypothesis that a persistent NLRP3 activation in macrophages was enhanced by Zol treatment, which might have contributed to impaired oral socket wound healing and associated increased incidence and severity of BRONJ-like diseae in *db/db* mice.

To date, much has been learned about NLRP3 inflammasome pathway activation, but the underlying mechanisms remain elusive. Currently, three models have been proposed for NLRP3 inflammasome activation, including exogenous ATP-induced K^+ efflux via P2X$_7$ receptor-gated ion channels, lysosomal disruption induced by phagocytosed large particles or crystals, and endogenous reactive oxygen species (ROS) generated by NADPH oxidases and/or mitochondria.[55] Interruption of ROS production by pharmacological inhibitors or scavengers inhibit NLRP3 inflammasome activation in response to many, if not all, previously evaluated activators, suggesting that ROS generation is a common upstream event required for NLRP3 activation.[55,56] Recent studies showed that statins induced caspase-1 activation and IL-1β release through ATP release, P2X$_7$ receptor activation, ROS generation, and lysosomal rupture.[32] In the present study, we have shown that blockade of K^+ channel and P2X$_7$ receptor and scavenging ROS production, but not lysosomal rupture, significantly abrogates Zol-enhanced IL-1β release in macrophages, suggesting that K^+/P2X$_7$ receptor/ROS pathway is involved in Zol-enhanced NLRP3 activation. However, the detailed molecular mechanisms underlying Zol-induced NLRP3 activation are warranted for further investigation.

In summary, we have demonstrated, for the first time to our knowledge, that macrophages at BRONJ-like lesions of *db/db* mice harbor an upregulated expression of NLRP3 inflammasome components and that Zol treatment augments the persistent NLRP3 activation in diabetic macrophages, which may have contributed to impaired oral socket wound healing and increased incidence and severity of BRONJ-like diseae in *db/db* mice. Therefore, further studies on how diabetes-associated NLRP3 activation affects oral wound healing have an enduring importance and can lead to novel and effective therapeutic modality for accelerating impaired oral wound healing in diabetic patients.

Disclosures

Acknowledgments

References

1. Reid IR, Cornish J. Epidemiology and pathogenesis of osteonecrosis of the jaw. Nat Rev Rheumatol. 2012;8(2):90–6.

2. Ruggiero SL, Dodson TB, Assael LA, et al. American Association of Oral and Maxillofacial Surgeons position paper on bisphosphonate-related osteonecrosis of the jaws—2009 update. J Oral Maxillofac Surg. 2009;67(5 Suppl):2–12.

3. Cetiner S, Sucak GT, Kahraman SA, et al. Osteonecrosis of the jaw in patients with multiple myeloma treated with zoledronic acid. J Bone Miner Metab. 2009;27(4):435–43.

4. Thumbigere-Math V, Tu L, Huckabay S, et al. A retrospective study evaluating frequency and risk factors of osteonecrosis of the jaw in 576 cancer patients receiving intravenous bisphosphonates. Am J Clin Oncol. 2012;35(4):386–92.

5. Sen CK, Gordillo GM, Roy S, et al. Human skin wounds: a major and snowballing threat to public health and the economy. Wound Repair Regen. 2009;17(6):763–71.

6. von Wilmowsky C, Stockmann P, Harsch I, et al. Diabetes mellitus negatively affects peri-implant bone formation in the diabetic domestic pig. J Clin Periodontol. 2011;38(8):771–9.

7. Wang F, Song YL, Li DH, et al. Type 2 diabetes mellitus impairs bone healing of dental implants in GK rats. Diabetes Res Clin Pract. 2010;88(1):e7–9.

8. Fang Y, Wang LP, Du FL, Liu WJ, Ren GL. Effects of insulin-like growth factor I on alveolar bone remodeling in diabetic rats. J Periodontal Res. 2013;48(2):144–50.

9. Lima SM, Grisi DC, Kogawa EM, et al. Diabetes mellitus and inflammatory pulpal and periapical disease: a review. Int Endod J. 2013;46(8):700–9.

10. Urade M. [Diabetes mellitus and bisphosphonate-related osteonecrosis of the jaws]. Clin Calcium. 2009;19(9):1332–8.

11. Molcho S, Peer A, Berg T, Futerman B, Khamaisi M. Diabetes microvascular disease and the risk for bisphosphonate-related osteonecrosis of the jaw: a single center study. J Clin Endocrinol Metab. 2013;98(11):E1807–12.

12. Berti-Couto SA, Vasconcelos AC, Iglesias JE, Figueiredo MA, Salum FG, Cherubini K. Diabetes mellitus and corticotherapy as risk factors for alendronate-related osteonecrosis of the jaws: a study in Wistar rats. Head Neck. 2014;36(1):84–93.

13. Khamaisi M, Regev E, Yarom N, et al. Possible association between diabetes and bisphosphonate-related jaw osteonecrosis. J Clin Endocrinol Metab. 2007;92(3):1172–5.

14. O'Ryan FS, Lo JC. Bisphosphonate-related osteonecrosis of the jaw in patients with oral bisphosphonate exposure: clinical course and outcomes. J Oral Maxillofac Surg. 2012;70(8):1844–53.

15. Schroder K, Tschopp J. The inflammasomes. Cell. 2010;140(6):821–32.

16. Artlett CM. Inflammasomes in wound healing and fibrosis. J Pathol. 2013;229(2):157–67.

17. Haneklaus M, O'Neill LA, Coll RC. Modulatory mechanisms controlling the NLRP3 inflammasome in inflammation: recent developments. Curr Opin Immunol. 2013;25(1):40–5.

18. Pelegrin P, Surprenant A. Dynamics of macrophage polarization reveal new mechanism to inhibit IL-1beta release through pyrophosphates. EMBO J. 2009;28(14):2114–27.

19. Martinez FO, Gordon S, Locati M, Mantovani A. Transcriptional profiling of the human monocyte-to-macrophage differentiation and polarization: new molecules and patterns of gene expression. J Immunol. 2006;177(10):7303–11.

20. Giulietti A, van Etten E, Overbergh L, Stoffels K, Bouillon R, Mathieu C. Monocytes from type 2 diabetic patients have a pro-inflammatory profile. 1,25-Dihydroxyvitamin D(3) works as anti-inflammatory. Diabetes Res Clin Pract. 2007;77(1):47–57.

21. Bradshaw EM, Raddassi K, Elyaman W, et al. Monocytes from patients with type 1 diabetes spontaneously secrete proinflammatory cytokines inducing Th17 cells. J Immunol. 2009;183(7):4432–9.

22. Mirza RE, Fang MM, Weinheimer-Haus EM, Ennis WJ, Koh TJ. Sustained inflammasome activity in macrophages impairs wound healing in type 2 diabetic humans and mice. Diabetes. 2014;63(3):1103–14.

23. Mirza RE, Fang MM, Ennis WJ, Koh TJ. Blocking interleukin-1beta induces a healing-associated wound macrophage phenotype and improves healing in type 2 diabetes. Diabetes. 2013;62(7):2579–87.

24. Mirza R, Koh TJ. Dysregulation of monocyte/macrophage phenotype in wounds of diabetic mice. Cytokine. 2011;56(2):256–64.

25. Thurnher M, Nussbaumer O, Gruenbacher G. Novel aspects of mevalonate pathway inhibitors as antitumor agents. Clin Cancer Res. 2012;18(13):3524–31.

26. Rogers TL, Holen I. Tumour macrophages as potential targets of bisphosphonates. J Transl Med. 2011;9:177.

27. Pazianas M. Osteonecrosis of the jaw and the role of macrophages. J Natl Cancer Inst. 2011;103(3):232–40.

28. Scheller EL, Hankenson KD, Reuben JS, Krebsbach PH. Zoledronic acid inhibits macrophage SOCS3 expression and enhances cytokine production. J Cell Biochem. 2011;112(11):3364–72.

29. Coscia M, Quaglino E, Iezzi M, et al. Zoledronic acid repolarizes tumour-associated macrophages and inhibits mammary carcinogenesis by targeting the mevalonate pathway. J Cell Mol Med. 2010;14(12):2803–15.

30. van der Burgh R, Ter Haar NM, Boes ML, Frenkel J. Mevalonate kinase deficiency, a metabolic autoinflammatory disease. Clin Immunol. 2013;147(3):197–206.

31. Xu JF, Washko GR, Nakahira K, et al. Statins and pulmonary fibrosis: the potential role of NLRP3 inflammasome activation. Am J Respir Crit Care Med. 2012;185(5):547–56.

32. Liao YH, Lin YC, Tsao ST, et al. HMG-CoA reductase inhibitors activate caspase-1 in human monocytes depending on ATP release and P2X7 activation. J Leukoc Biol. 2013;93(2):289–99.

33. Kuijk LM, Mandey SH, Schellens I, et al. Statin synergizes with LPS to induce IL-1beta release by THP-1 cells through activation of caspase-1. Mol Immunol. 2008;45(8):2158–65.

34. Deng X, Tamai R, Endo Y, Kiyoura Y. Alendronate augments interleukin-1beta release from macrophages infected with periodontal pathogenic bacteria through activation of caspase-1. Toxicol Appl Pharmacol. 2009;235(1):97–104.

35. Pontillo A, Paoluzzi E, Crovella S. The inhibition of mevalonate pathway induces upregulation of NALP3 expression: new insight in the pathogenesis of mevalonate kinase deficiency. Eur J Hum Genet. 2010;18(7):844–7.

36. Zhang Q, Atsuta I, Liu S, et al. IL-17-mediated M1/M2 macrophage alteration contributes to pathogenesis of bisphosphonate-related osteonecrosis of the jaws. Clin Cancer Res. 2013;19(12):3176–88.

37. Kikuiri T, Kim I, Yamaza T, et al. Cell-based immunotherapy with mesenchymal stem cells cures bisphosphonate-related osteonecrosis of the jaw-like disease in mice. J Bone Miner Res. 2010;25(7):1668–79.

38. Koh GC, Weehuizen TA, Breitbach K, et al. Glyburide reduces bacterial dissemination in a mouse model of melioidosis. PLoS Negl Trop Dis. 2013;7(10):e2500.

39. Munoz-Planillo R, Kuffa P, Martinez-Colon G, Smith BL, Rajendiran TM, Nunez G. K(+) efflux is the common trigger of NLRP3 inflammasome activation by bacterial toxins and particulate matter. Immunity. 2013;38(6):1142–53.

40. Lamkanfi M, Mueller JL, Vitari AC, et al. Glyburide inhibits the Cryopyrin/Nalp3 inflammasome. J Cell Biol. 2009;187(1):61–70.

41. Nussbaumer O, Gruenbacher G, Gander H, Thurnher M. DC-like cell-dependent activation of human natural killer cells by the bisphosphonate zoledronic acid is regulated by gammadelta T lymphocytes. Blood. 2011;118(10):2743–51.

42. Ruggiero SL, Dodson TB, Fantasia J, et al. American Association of Oral and Maxillofacial Surgeons position paper on medication-related osteonecrosis of the jaw—2014 update. J Oral Maxillofac Surg. 2014;72(10):1938–56.

43. Kimmel DB. Mechanism of action, pharmacokinetic and pharmaco-dynamic profile, and clinical applications of nitrogen-containing bisphosphonates. J Dent Res. 2007;86(11):1022–33.

44. Silva I, Branco JC. Denosumab: recent update in postmenopausal osteoporosis. Acta Reumatol Port. 2012;37(4):302–13.

45. Kostenuik PJ, Nguyen HQ, McCabe J, et al. Denosumab, a fully human monoclonal antibody to RANKL, inhibits bone resorption and increases BMD in knock-in mice that express chimeric (murine/human) RANKL. J Bone Miner Res. 2009;24(2):182–95.

46. de Molon RS, Shimamoto H, Bezouglaia O, et al. OPG-Fc but not zoledronic acid discontinuation reverses osteonecrosis of the jaws (ONJ) in mice. J Bone Miner Res. Epub 2015 Feb 28. DOI: 10.1002/jbmr.2490

47. Novak ML, Koh TJ. Phenotypic transitions of macrophages orchestrate tissue repair. Am J Pathol. 2013;183(5):1352–63.

48. Lucas T, Waisman A, Ranjan R, et al. Differential roles of macrophages in diverse phases of skin repair. J Immunol. 2010;184(7):3964–77.

49. Jesus AA, Goldbach-Mansky R. IL-1 blockade in autoinflammatory syndromes. Annu Rev Med. 2014;65:223–44.

50. Gris D, Ye Z, Iocca HA, et al. NLRP3 plays a critical role in the development of experimental autoimmune encephalomyelitis by mediating Th1 and Th17 responses. J Immunol. 2010;185(2):974–81.

51. Meng G, Zhang F, Fuss I, Kitani A, Strober W. A mutation in the Nlrp3 gene causing inflammasome hyperactivation potentiates Th17 cell-dominant immune responses. Immunity. 2009;30(6):860–74.

52. Bruchard M, Mignot G, Derangere V, et al. Chemotherapy-triggered cathepsin B release in myeloid-derived suppressor cells activates the Nlrp3 inflammasome and promotes tumor growth. Nat Med. 2013;19(1):57–64.

53. Thurnher M, Nussbaumer O, Gruenbacher G. Novel aspects of mevalonate pathway inhibitors as antitumor agents. Clin Cancer Res. 2012;18(13):3524–31.

54. Vandebriel RJ, De Jong HJ, Gremmer ER, et al. Statins accelerate the onset of collagen type II-induced arthritis in mice. Arthritis Res Ther. 2012;14(2):R90.

55. Zhou R, Yazdi AS, Menu P, Tschopp J. A role for mitochondria in NLRP3 inflammasome activation. Nature. 2011;469(7329):221–5.

56. Iyer SS, He Q, Janczy JR, et al. Mitochondrial cardiolipin is required for Nlrp3 inflammasome activation. Immunity. 2013;39(2):311–23.